

Injection locking-based pump recovery for phase-sensitive amplified links

Samuel L. I. Olsson,^{1,*} Bill Corcoran,¹ Carl Lundström,¹ Ekawit Tipsuwannakul,¹ Stylianos Sygletos,^{2,3} Andrew D. Ellis,^{2,3} Zhi Tong,^{1,4} Magnus Karlsson,¹ and Peter A. Andrekson¹

¹Photonics Laboratory, Department of Microtechnology and Nanoscience, Chalmers University of Technology, SE-412 96, Gothenburg, Sweden

²Tyndall National Institute and Department of Physics, University College Cork, Ireland

³Now at: Aston Institute of Photonic Technologies, Aston University, Birmingham, B4 7ET, UK

⁴Now at: Department of Electrical and Computer Engineering, University of California San Diego, La Jolla, CA 92093, USA

*samuel.olsson@chalmers.se

Abstract: An injection locking-based pump recovery system for phase-sensitive amplified links, capable of handling 40 dB effective span loss, is demonstrated. Measurements with 10 GBd DQPSK signals show penalty-free recovery of a pump wave, phase modulated with two sinusoidal RF-tones at 0.1 GHz and 0.3 GHz, with 64 dB amplification. The operating power limit for the pump recovery system is experimentally investigated and is governed by the noise transfer and phase modulation transfer characteristics of the injection-locked laser. The corresponding link penalties are explained and quantified. This system enables, for the first time, WDM compatible phase-sensitive amplified links over significant lengths.

© 2013 Optical Society of America

OCIS codes: (060.2320) Fiber optics amplifiers and oscillators; (140.3520) Lasers, injection-locked.

References and links

1. C. M. Caves, "Quantum limits on noise in linear amplifiers," *Phys. Rev. D* **26**, 1817–1839 (1982).
2. E. Desurvire, *Erbium-doped Fiber Amplifiers*, (John Wiley & Sons, 1994).
3. W. Imajuku, A. Takada, and Y. Yamabayashi, "Low-noise amplification under the 3dB noise figure in high-gain phase-sensitive fibre amplifier," *Electron. Lett* **35**, 1954–1955 (1999).
4. D. J. Lovering, J. A. Levenson, P. Vidakovic, J. Webjörn, and P. St. J. Russell, "Noiseless optical amplification in quasi-phase-matched bulk lithium niobate," *Opt. Lett.* **21**, 1439–1441 (1996).
5. Z. Tong, C. Lundström, P. A. Andrekson, C. J. McKinstry, M. Karlsson, D. J. Blessing, E. Tipsuwannakul, B. J. Puttnam, H. Toda, and L. Grüner-Nielsen, "Towards ultrasensitive optical links enabled by low-noise phase-sensitive amplifiers," *Nat. Photonics* **5**, 430–436 (2011).
6. J. Hansryd, P. A. Andrekson, M. Westlund, J. Li, and P. O. Hedekvist, "Fiber-Based Optical Parametric Amplifiers and Their Applications," *IEEE J. Sel. Topics Quantum Electron.* **8**, 506–520 (2002).
7. J. Kakande, C. Lundström, P. A. Andrekson, Z. Tong, M. Karlsson, P. Petropoulos, F. Parmigiani, and D. J. Richardson, "Detailed characterization of a fiber-optic parametric amplifier in phase-sensitive and phase-insensitive operation," *Opt. Express* **18**, 4130–4137 (2010).
8. M. Vasilyev, "Distributed phase-sensitive amplification," *Opt. Express* **13**, 7563–7571 (2005).
9. R. Tang, P. Devgan, V. S. Grigoryan, and P. Kumar, "Inline frequency-non-degenerate phase-sensitive fibre parametric amplifier for fibre-optic communication," *Electron. Lett* **41**, 1072–1074 (2005).
10. R. Tang, P. Devgan, P. L. Voss, V. S. Grigoryan, and P. Kumar, "In-Line Frequency-Nondegenerate Phase-Sensitive Fiber-Optical Parametric Amplifier," *IEEE Photon. Technol. Lett.* **17**, 1845–1847 (2005).
11. O. K. Lim, V. Grigoryan, M. Shin, and P. Kumar, "Ultra-Low-Noise Inline Fiber-Optic Phase-Sensitive Amplifier for Analog Optical Signals," in *Optical Fiber Communication Conference and Exposition (OFC) and National*

- Fiber Optic Engineers Conference (NFOEC)*, Technical Digest (CD) (Optical Society of America, 2008), paper OML3.
12. R. Tang, J. Lasri, P. S. Devgan, V. Grigoryan, P. Kumar, and M. Vasilyev, "Gain characteristics of a frequency nondegenerate phase-sensitive fiber-optic parametric amplifier with phase self-stabilized input," *Opt. Express* **13**, 10483–10493 (2005).
 13. Z. Tong, C. J. McKinstrie, C. Lundström, M. Karlsson, and P. A. Andrekson, "Noise performance of optical fiber transmission links that use non-degenerate cascaded phase-sensitive amplifiers," *Opt. Express* **18**, 15426–15439 (2010).
 14. C. J. McKinstrie, M. Karlsson, and Z. Tong, "Field-quadrature and photon-number correlations produced by parametric processes," *Opt. Express* **18**, 19792–19823 (2010).
 15. Z. Tong, C. Lundström, E. Tipsuwannakul, M. Karlsson, and P. A. Andrekson, "Phase-Sensitive Amplified DWDM DQPSK Signals Using Free-Running Lasers with 6-dB Link SNR Improvement over EDFA-based Systems," in *European Conference and Exhibition on Optical Communication (ECOC)*, Technical Digest (CD) (Optical Society of America, 2010), paper PDP1.3.
 16. Z. Tong, C. Lundström, P. A. Andrekson, M. Karlsson, and A. Bogris, "Ultralow Noise, Broadband Phase-Sensitive Optical Amplifiers, and Their Applications," *IEEE J. Sel. Topics Quantum Electron.* **18**, 1016–1032 (2012).
 17. Z. Tong, A. Bogris, C. Lundström, C. J. McKinstrie, M. Vasilyev, M. Karlsson, and P. A. Andrekson, "Modeling and measurement of the noise figure of a cascaded non-degenerate phase-sensitive parametric amplifier," *Opt. Express* **18**, 14820–14835 (2010).
 18. A. Takada and W. Imajuku, "Optical phase-sensitive amplifier with pump laser phase-locked to input signal light," in *Proceedings of European Conference and Exhibition on Optical Communication (ECOC)*, (Optical Society of America, 1997), 98–101.
 19. R. Slavík, F. Parmigiani, J. Kakande, C. Lundström, M. Sjödin, P. A. Andrekson, R. Weerasuriya, S. Sygletos, A. D. Ellis, L. Grüner-Nielsen, D. Jakobsen, S. Herstrøm, R. Phelan, J. O'Gorman, A. Bogris, D. Syvridis, S. Dasgupta, P. Petropoulos, and D. J. Richardson, "All-optical phase and amplitude regenerator for next-generation telecommunications systems," *Nat. Photonics* **4**, 690–695 (2010).
 20. S. Sygletos, R. Weerasuriya, S. K. Ibrahim, F. Gunning, R. Phelan, J. O'Gorman, J. O'Carroll, B. Kelly, A. Bogris, D. Syvridis, C. Lundström, P. Andrekson, F. Parmigiani, D. J. Richardson, and A. D. Ellis, "Phase Locking and Carrier Extraction Schemes for Phase Sensitive Amplification," in *Conference on Transparent Optical Networks (ICTON), 2010 12th International*, Technical Digest (CD) (Optical Society of America, 2010), paper Mo.C1.3.
 21. S. Kasapi, S. Lathi, and Y. Yamamoto, "Amplitude-squeezed, frequency-modulated, tunable, diode-laser-based source for sub-shot-noise FM spectroscopy," *Opt. Lett.* **22**, 478–480 (1997).
 22. E. K. Lau, L. J. Wong, X. Zhao, Y. K. Chen, C. J. Chang-Hasnain, and M. C. Wu, "Bandwidth Enhancement by Master Modulation of Optical Injection-Locked Lasers," *J. Lightw. Technol.* **26**, 2584–2593 (2008).
 23. A. Fragkos, A. Bogris, D. Syvridis, and R. Phelan, "Amplitude Noise Limiting Amplifier for Phase Encoded Signals Using Injection Locking in Semiconductor Lasers," *J. Lightw. Technol.* **30**, 764–771 (2012).
 24. E. K. Lau and M. C. Wu, "Amplitude and Frequency Modulation of the Master Laser in Injection-Locked Laser Systems," in *Proceedings of International Topical Meeting on Microwave Photonics*, (2004), 142–145.
 25. M. Vainio, M. Merimaa, and K. Nyholm, "Modulation transfer characteristics of injection-locked diode lasers," *Opt. Commun.* **267**, 455–463 (2006).
 26. S. L. I. Olsson, B. Corcoran, C. Lundström, E. Tipsuwannakul, S. Sygletos, A. D. Ellis, Z. Tong, M. Karlsson, and P. A. Andrekson, "Optical Injection-Locking-Based Pump Recovery for Phase-Sensitively Amplified Links," in *Optical Fiber Communication Conference and Exposition (OFC) and National Fiber Optic Engineers Conference (NFOEC)*, Technical Digest (CD) (Optical Society of America, 2012), paper OW3C.3.
 27. B. Corcoran, S. L. I. Olsson, C. Lundström, M. Karlsson, and P. Andrekson, "Phase-sensitive Optical Pre-Amplifier Implemented in an 80km DQPSK Link," in *Optical Fiber Communication Conference and Exposition (OFC) and National Fiber Optic Engineers Conference (NFOEC)*, Technical Digest (CD) (Optical Society of America, 2012), paper PDP5A.4.
 28. S. L. I. Olsson, B. Corcoran, C. Lundström, M. Sjödin, M. Karlsson, and P. A. Andrekson, "Phase-Sensitive Amplified Optical Link Operating in the Nonlinear Transmission Regime," in *European Conference and Exhibition on Optical Communication (ECOC)*, Technical Digest (CD) (Optical Society of America, 2012), paper Th.2.F.1.
 29. S. K. Korotky, P. B. Hansen, L. Eskildsen, and J. J. Veselka, "Efficient phase modulation scheme for suppressing stimulated Brillouin scattering," in *Proc. Technol. Dig. Conf. Integr. Opt. Fiber Commun.*, (1995), 110–111.
 30. A. Furusawa, "Amplitude squeezing of a semiconductor laser with light injection," *Opt. Lett.* **21**, 2014–2016 (1996).
 31. C. Lundström, R. Malik, L. Grüner-Nielsen, B. Corcoran, S. L. I. Olsson, M. Karlsson, and P. A. Andrekson, "Fiber Optic Parametric Amplifier With 10-dB Net Gain Without Pump Dithering," *IEEE Photon. Technol. Lett.* **25**, 234–237 (2013).

1. Introduction

Phase-sensitive amplifiers (PSAs), e.g. fiber optic parametric amplifiers (FOPAs) in phase-sensitive (PS)-mode, are in theory capable of noiseless amplification, i.e. a 0 dB noise figure (NF) [1]. This should be compared with phase-insensitive amplifiers (PIAs) such as erbium-doped fiber amplifiers (EDFAs) having a 3 dB quantum-limited NF at high gain [2]. Low NF PSAs have been realized in both FOPAs [3], and nonlinear crystals [4], with FOPA-based implementations showing significantly higher gain. A high-gain optical amplifier with close to 0 dB NF would have major impact on areas such as sensing and spectroscopy as well as fiber optical communication systems [5].

FOPA PSAs require in their simplest configuration three frequency- and phase-locked waves at the input, commonly referred to as pump, signal, and idler, and can be implemented in frequency-degenerate and frequency-nondegenerate configurations. Frequency-degenerate PSAs can only amplify one specific wavelength channel for a given pump configuration and are difficult to implement with high gain due to the quadratic dependence of the gain on the pump power [6]. Frequency-nondegenerate PSAs on the other hand support simultaneous amplification of many independent signals and can provide high gain, growing exponentially with pump power [7].

The concept of a frequency-nondegenerate PSA-amplified transmission link, utilizing the ultra-low NF, multi-channel capability, and high gain of a frequency-nondegenerate PSA, was first introduced in 2005 by Vasilyev et al. [8]. The first experimental realization of a frequency-nondegenerate PSA-amplified transmission link was using single-channel 2.5 Gbit/s non-return-to-zero (NRZ) data transmitted over a 60 km dispersion compensated link [9]. The frequency- and phase-locking of the waves was accomplished using an optical double-sideband modulation scheme [10, 11], with the bandwidth limited to the bandwidth of the optical modulators used to generate the sidebands. Following demonstrations have used an all-optical scheme which is based on four-wave mixing (FWM) where the frequency- and phase-locking is achieved through parametric idler creation. The combination of a PIA, for creating a set of frequency- and phase-locked waves, followed by a PSA, is a practical way of implementing a PSA and was first introduced in [12]. This scheme is commonly referred to as the copier-PSA scheme.

The copier-PSA scheme has been thoroughly investigated and it has been shown theoretically that a transmission link implementation of the scheme can give up to 6 dB link NF improvement over conventional PIA-based schemes and a 3 dB improvement over all PSA-based schemes [13, 14]. This has also been shown experimentally for a copier-loss-PSA system, where the link was emulated by a lumped signal/idler loss [5]. Based on the copier-loss-PSA system, amplification of dense wavelength division multiplexed (DWDM) differential quadrature phase-shift keyed (DQPSK) signals at 10 GBd with nearly 6 dB signal-to-noise ratio (SNR) improvement over an EDFA-based system have been demonstrated [15, 16]. This demonstration showed input signal-format independence and DWDM channel amplification capability of the copier-PSA scheme, two features very important for communication links.

A schematic illustration of a transmission link with lumped PSA amplification, based on the copier-PSA scheme, is shown in Fig. 1. A signal wave encoded with data along with a high-power pump wave, possibly phase modulated for suppression of stimulated Brillouin scattering (SBS), are injected into the copier. The copier is implemented with a PI-FOPA and when passing through the copier an idler wave, frequency- and phase-locked to the signal and pump, is created via FWM. Before transmission the high-power pump wave is separated from the signal/idler pair and attenuated to avoid degrading nonlinear effects such as cross-phase modulation (XPM) and self-phase modulation (SPM) during transmission and the signal/idler waves are tuned with respect to phase, delay, and dispersion. After recombining the pump with the

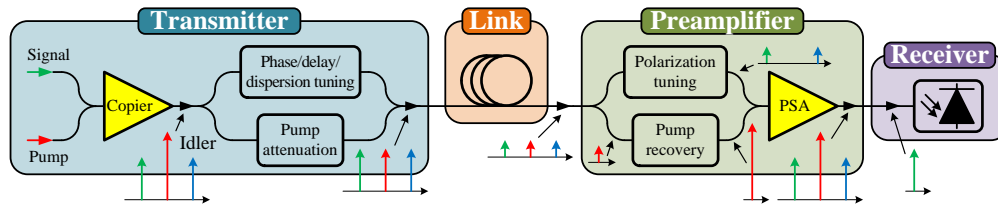


Fig. 1. Schematic illustration of a phase-sensitive amplified (PSA) transmission link based on the copier-PSA scheme.

signal/idler pair the waves are sent through the transmission link.

After transmission the pump is separated from the signal/idler pair and led through a pump recovery system. The pump recovery system should produce a high-quality pump wave based on the residual pump wave after transmission and is essential for obtaining the benefits of a PSA-amplified link. The signal and idler polarizations are tuned to maximize the PSA gain. The waves are then recombined and led into the PSA, implemented by a PS-FOPA, where low NF amplification takes place before the signal wave is filtered out and detected by the receiver. It is critical that the noise added on the signal and idler waves in the copier is decorrelated before the PSA for low NF PSA operation to be possible [17]. In the transmission link implementation of the copier-PSA scheme this is achieved by the loss in the link.

Previous demonstrations of PSA-amplified links have not adequately considered the pump recovery system. In [9] the pump recovery before the PSA was achieved using a single EDFA and possible penalty due to pump degradation through the pump recovery was not considered. As mentioned earlier, the experimental work presented in [5, 15, 16] was carried out with a lumped signal/idler loss instead of transmission link and thus no pump attenuation stage or pump recovery system was used or required in those demonstrations. As such, pump recovery has provided a major obstacle in implementing a PSA-amplified link over significant fiber spans.

Pump recovery can be accomplished using optical injection locking (IL). There have been several demonstrations of pump wave generation, using IL, for subsequent use in PSAs. However, not in the context of frequency-nondegenerate PSA-amplified transmission links. IL has been used for phase-locking a semiconductor ring laser to a pulsed signal that was used as pump in an in-line frequency-degenerate PSA [18]. An all-optical regenerator has been demonstrated where IL was used for narrowband filtering of a generated carrier wave and the injection-locked wave later used as pump in a saturated PSA [19]. Two schemes, both using IL, have been demonstrated for generating phase-locked pump waves for use in in-line “black-box” frequency-nondegenerate PSAs [20].

IL has also proved to be an extremely useful technique in a number of areas and has been thoroughly investigated for applications such as FM spectroscopy [21], and modulation bandwidth enhancement [22]. There has also been a number of theoretical and experimental investigations dedicated to amplitude modulation (AM) and frequency modulation (FM) transfer for various operating regimes and slave laser (SL) driving conditions [23–25]. However, to the best of our knowledge, no detailed investigation of amplified spontaneous emission (ASE) noise transfer through an injection-locked distributed feedback (DFB) laser has previously been published, with only power spectral density measurements performed of the output of a semiconductor laser injection-locked to an ASE degraded signal [23].

The first demonstration of a nontrivial pump recovery system for frequency-nondegenerate PSA-amplified links was presented in [26]. This system enabled the demonstration of an 80 km PSA-amplified transmission link [27], the longest frequency-nondegenerate PSA-amplified

link ever reported. The pump recovery system also enabled an investigation of transmission in the nonlinear regime [28].

In this paper we extend the concept presented in [26]. Apart from demonstrating penalty-free operation of a PSA-amplified link, with phase modulated pump, for equivalent link losses of more than 40 dB we also present the first detailed experimental investigation of the operating power limits of the pump recovery system. We measure the noise generation in and the phase modulation transfer through the pump recovery system and relate this to bit error ratio (BER) measurements which enables us to understand the penalty mechanisms and draw conclusions about how the system can be improved. The investigation also contains novel measurement results on ASE noise transfer through an injection-locked DFB laser.

The paper is organized as follows. In section 2 we demonstrate our proposed pump recovery system in a PSA- and a PIA-amplified link for equivalent link lengths of up to 50 dB loss which let us observe the operating power limits. In section 3 we investigate in detail the factors that determine the operating limits, i.e. noise generation in and phase modulation transfer through the pump recovery system. Then in section 4, the measurements in section 3 are related to the PSA/PIA-amplified link performance and conclusions are drawn regarding how the pump recovery system performance can be improved. Finally in section 5 we state our conclusions.

2. The pump recovery scheme and demonstration

To get an idea of the requirements on a pump recovery system in a PSA-amplified link we consider a specific case as an example. We start with the condition that the pump power into the transmission link should not exceed 10 dBm. It has been shown that this level of pump power does not degrade the performance of a PSA-amplified 80 km link [27]. If our target is a 100 km link then the pump will be attenuated by about 20 dB through the link. Furthermore, if we aim at 20 dB PSA net gain, then in our PSA implementation approximately 34 dBm of pump power is needed at the PSA input. With these limitations we need about 44 dB pump amplification in the pump recovery system. Apart from the high amplification, the recovered pump must also have high OSNR to avoid penalty from pump transfer noise in the PSA and we additionally require phase information on the incoming pump wave to be correctly reproduced since in our experiments we use a phase modulated pump for suppression of SBS [29]. These requirements on amplification and OSNR are impossible to satisfy using ordinary EDFAs and thus a different solution is required.

The pump recovery system which we demonstrate here is a hybrid IL/EDFA solution where IL is used for its amplification, filtering, and amplitude squeezing properties [30], and the EDFAs for power amplification. We demonstrate the performance and the operating power limits of the pump recovery system by carrying out BER measurements on a PSA-amplified link incorporating the pump recovery system. To gain further insight we compare the performance with the same system operated in PI-mode (by blocking the idler after the copier) and an EDFA-amplified link. We also compare the performance of the hybrid IL/EDFA pump recovery system with a simple EDFA-based system, obtained by bypassing the IL in the hybrid system. Our link does not include any transmission fiber, instead the link loss is emulated by a lumped loss element.

2.1. Experimental setup

The experimental setup is shown in Fig. 2. A signal wave at 1545.2 nm was encoded with a 10 GBd DQPSK $2^{15} - 1$ pseudorandom bit sequence (PRBS). The signal was combined, using a wavelength division multiplexer (WDM), with a high-power pump wave at 1553.7 nm, phase modulated with two sinusoidal radio frequency (RF)-tones at 0.1 GHz and 0.3 GHz (giving 0.8 GHz bandwidth) for suppression of SBS in the FOPAs.

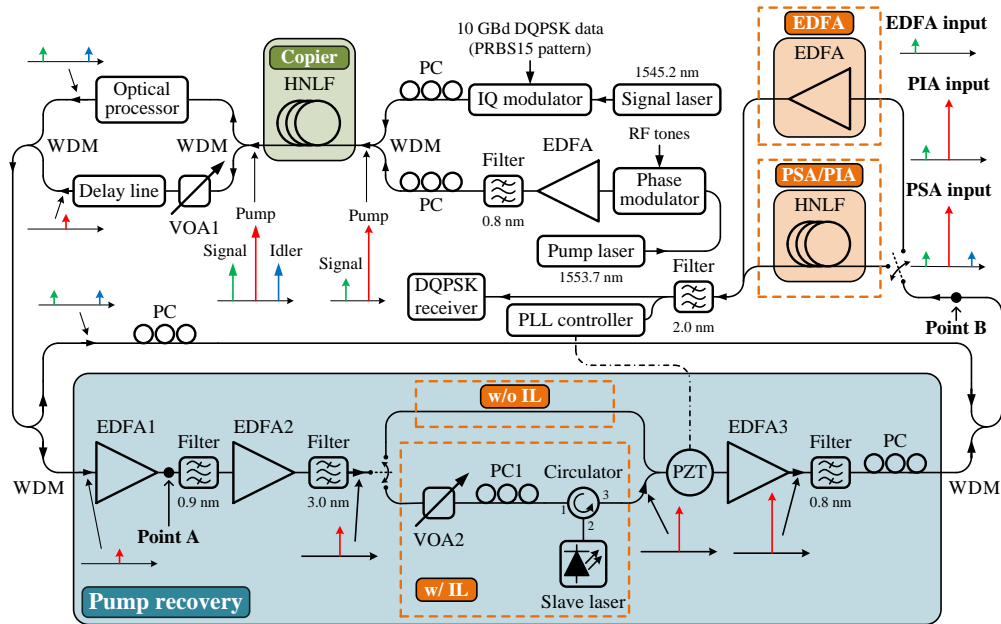


Fig. 2. Experimental setup used for demonstration and bit error ratio characterization of an injection locking-based pump recovery system in a phase-sensitive amplified link. DQPSK: differential quadrature phase-shift keyed, PRBS: pseudorandom bit sequence, RF: radio frequency, PC: polarization controller, WDM: wavelength division multiplexer, HNLF: highly nonlinear fiber, VOA: variable optical attenuator, EDFA: erbium-doped fiber amplifier, IL: injection locking, PZT: piezoelectric transducer, PSA: phase-sensitive amplifier, PIA: phase-insensitive amplifier, BER: bit error ratio, PLL: phase-locked loop.

The two waves were launched into the copier, consisting of 250 m highly nonlinear fiber (HNLF) with zero dispersion wavelength $\lambda_0 = 1545$ nm, and a phase-conjugated copy of the signal, the idler, was generated at 1562.2 nm through FWM. The copier had no net gain and the signal was 8.5 dB stronger than the idler at the output. The signal and idler waves were then separated from the pump wave and lead through an optical processor (OP) for power attenuation and equalization, filtering, and signal-idler relative delay tuning. The OP was also used for switching between PS- and PI-mode by selectively blocking the idler. The pump wave was attenuated using a variable optical attenuator (VOA), VOA1, to emulate link loss and vary the pump OSNR at point A. A delay line matched the optical path length for the signal/idler and pump waves.

After recombining the pump with the signal/idler pair they were again separated and the signal/idler pair was passed through a polarization controller (PC) while the pump was passed through the pump recovery system. The pump OSNR at the input of the pump recovery system was > 60 dB. The signal/idler pair was attenuated by more than 20 dB between the copier and the PSA/PIA preamplifier for all measurements which should be enough to decorrelate the signal/idler noise added in the copier.

In the pump recovery system the pump wave was first amplified by two EDFAs, EDFA1 and EDFA2, followed by a 0.9 nm and a 3.0 nm bandpass filter respectively. For the case with IL the pump wave was passed through VOA2 for tuning the power into the SL and then through PC1 for controlling the state of polarization (SOP). The SOP was tuned so that the phase transfer through the SL was maximized. The wave was then, via a circulator, injected into the SL which

was a DFB laser without isolator. The SL input power was re-optimized for lowest BER at each setting of VOA1. The SL driving current was seven times the lasing threshold value, giving an output power of 20 dBm, and its wavelength was tuned so that the frequency difference between the SL and the incoming wave was minimized. For the case without IL the pump wave was passed unaffected through another path, as indicated in Fig. 2. The pump was finally amplified to 33.8 dBm for the PSA-amplified link and to 34.9 dBm for the PIA-amplified link and filtered by a 0.8 nm bandpass filter. The relative phase between the pump and signal/idler pair was stabilized from thermal drift and acoustic noise using a phase-locked loop (PLL) based on a frequency dither technique. The frequency dithering was applied using a piezoelectric transducer (PZT)-based fiber stretcher placed in the pump path of the pump recovery system.

The PSA/PIA preamplifier was implemented with two cascaded spools of stretched Ge-doped HNLF with an isolator in between for SBS suppression [31]. The gain was 20 dB both in the PSA- and PIA-case and was tuned by varying the output power from EDFA3. For the PSA-case the signal and idler powers launched into the preamplifier were equal. The FOPA preamplifiers were compared against an EDFA preamplifier with 3.8 dB NF, also with 20 dB gain. PCs were used to align the SOP of the waves before the FOPAs.

For the BER measurements the received signal power was measured at point B and varied using the OP. The preamplifier output was passed through a 2.0 nm bandpass filter and then into the differential receiver, comprising of a 1-bit delay interferometer and an amplified balanced receiver. Although only one branch of the DQPSK signal was demodulated and used for BER measurement, it has been previously shown that for copier-PSA schemes both tributaries perform similarly [15]. Part of the filtered signal was diverted and used as a feedback signal for the PLL.

2.2. Measurement results

Measurement results showing BER versus received signal power, i.e. signal power measured at point B, are presented in Fig. 3. For each of our three preamplifier configurations, with or without IL in the pump recovery system, we compare operation at different pump OSNR at point A.

At high pump OSNR (56 dB), we observe all systems operating as expected, with a 4.8 dB sensitivity increase comparing the PIA- and PSA-amplified cases. This is close to the ideal 6 dB improvement expected through the lower NF of the PSA [16].

When lowering pump OSNR from 56 dB to 37 dB, both the PIA- and PSA-amplified systems show a large sensitivity penalty when IL is not used in the pump recovery system. With IL in place, both the PIA- and PSA-amplified systems show much improved performance. However, significant penalty is observed when the pump OSNR is degraded to 11 dB.

To analyze how this sensitivity penalty evolves in our different systems, we plot the Q-factor penalty versus pump OSNR at point A. The Q-factor was calculated from measured BER using: $Q = 20 \log_{10}[\sqrt{2} \operatorname{erf}^{-1}(2\text{BER})]$. For the PSA-case, the penalty was taken with respect to the performance at -42 dBm received signal power at 56 dB pump OSNR giving a BER of about 10^{-8} . For the PIA-case the penalty was taken with respect to the performance at -37 dBm received signal power at 56 dB pump OSNR also giving a BER of about 10^{-8} . The measurements were done with the pump recovery system optimized for each measurement point.

The Q-factor penalty versus pump OSNR at point A (bottom axis) and pump power at the pump recovery system input (top axis) is plotted in Fig. 4. As the pump OSNR is decreased, we see the Q-factor penalty increases, while showing the systems without IL penalized more heavily, as in Fig. 3. For the systems without IL, this penalty becomes apparent at a pump OSNR of about 50 dB, corresponding to roughly 0 dBm pump power at the input of the pump recovery

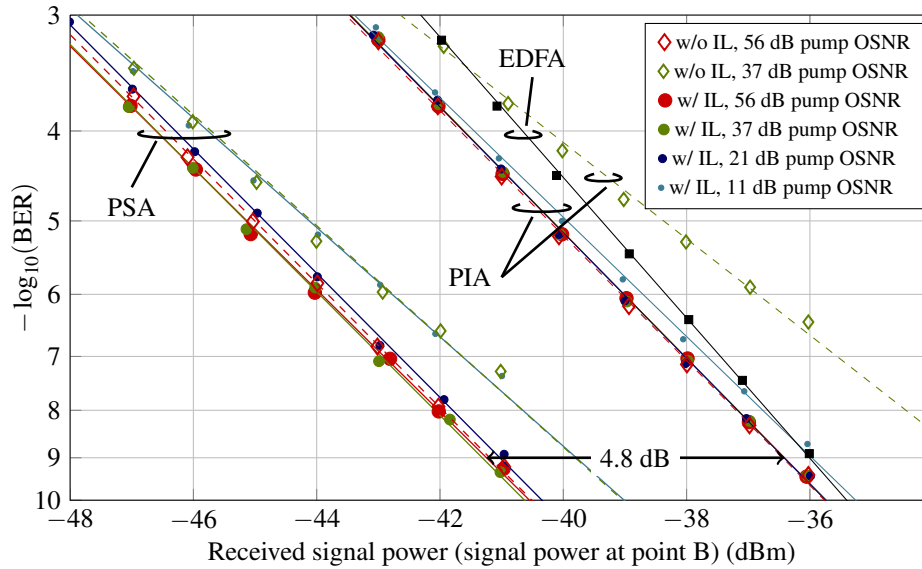


Fig. 3. Measured bit error ratio (BER) versus received signal power (signal power at point B) comparing a phase-insensitive amplifier (PIA) and a phase-sensitive amplifier (PSA) amplified receiver with and without injection locking (IL) in the pump recovery system with an erbium-doped fiber amplifier (EDFA) amplified receiver. The measurements were done at various pump optical signal-to-noise ratio (OSNR) at point A, as given by the legend. The straight lines are linear fittings to the measurement points.

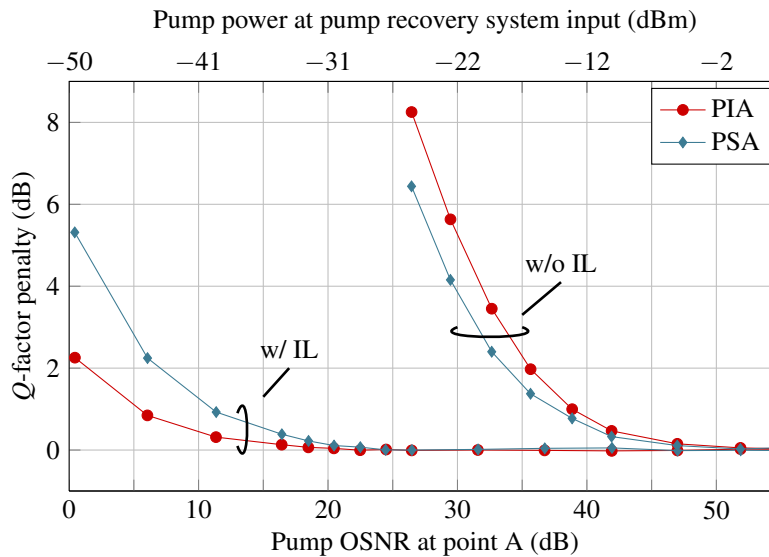


Fig. 4. Q-factor penalty calculated from measured bit error ratio versus pump optical signal-to-noise ratio (OSNR) at point A (bottom axis) and pump power at the pump recovery system input (top axis) comparing a phase-insensitive amplifier (PIA) and phase-sensitive amplifier (PSA) amplified receiver with and without injection locking (IL) in the pump recovery system.

system. For the systems with IL, penalty-free operation is observed down to a pump OSNR of 20 dB, corresponding to about -30 dBm pump power at the input of the pump recovery system.

We can conclude that our proposed hybrid IL/EDFA pump recovery system show penalty-free operation in a PSA-amplified link with lumped loss where the pump is phase modulated by two sinusoidal RF-tones at 0.1 GHz and 0.3 GHz (giving a 0.8 GHz bandwidth) and experience 64 dB overall amplification, from -30 dBm to 34 dBm. With the assumption of 10 dBm pump power launched into the link the penalty onset at 20 dB pump OSNR corresponds to a link attenuation of 40 dB.

Replacing the 40 dB lumped loss with a 200 km dispersion compensated fiber span will introduce nonlinear and linear effects that can degrade the pump wave and give additional penalties, i.e. shift the pump recovery penalty onset to a higher pump OSNR. However, as we will outline below, we believe that these effects are negligible given that the pump power launched into the link is low enough and that the bandwidth of the pump, dominated by the pump phase modulation, is small. That the transmission related penalties for the pump recovery system are negligible in our system has also been shown experimentally for an 80 km link with 10 dBm pump power launched into the link [27].

The dominant nonlinear effect acting on the pump wave will be SPM, which would add phase distortions. The impact of SPM can be estimated by calculating the nonlinear phase shift Φ . Using standard single mode fiber (SSMF), with attenuation $\alpha = 0.2$ dB km $^{-1}$ and nonlinear coefficient $\gamma = 1$ W $^{-1}$ km $^{-1}$, the nonlinear phase shift for $P_0 = 10$ dBm power launched into a $L = 200$ km long fiber is $\Phi = \gamma P_0 [1 - \exp(-\alpha L)] / \alpha = 0.064\pi$. The small nonlinear phase shift along with the continuous wave (CW) nature of the pump wave suggest that there should be no significant penalty related to SPM.

In a dispersion compensated link chromatic dispersion related effects such as phase to amplitude conversion will not cause any penalty. The dominant linear effect will instead be polarization mode dispersion (PMD), which could cause issues with polarization alignment for the IL process. Using the frequency-domain manifestation of PMD we can relate the output phase $\phi = \Delta\beta L$, where $\Delta\beta = \beta_{\text{slow}} - \beta_{\text{fast}}$ is the propagation constant difference between the fast and the slow axis, to the bandwidth $\Delta\omega$ of the pump wave. The change in output phase $\Delta\phi$ is related to $\Delta\omega$ by $\Delta\phi = \Delta\omega\Delta\tau$ where $\Delta\tau$ is the root mean square (RMS) value of the differential group delay (DGD) of the fiber. The DGD can be calculated from $\Delta\tau = D_p L^{1/2}$ where D_p is the PMD parameter, which is typically around 0.1 ps km $^{-1}$ in modern fibers. Using the spectral width of the phase modulated pump wave $\Delta f = 0.8$ GHz and a $L = 200$ km long fiber we get an output phase difference of $\Delta\phi = 2\pi\Delta f D_p L^{1/2} = 4.5 \times 10^{-3}$, which is negligible.

3. Investigation of pump recovery system operation limits

In the previous section we observed a large Q-factor penalty for the PSA/PIA-amplified systems as the power reaching the pump recovery system was decreased. To understand what is causing the penalty and how the pump recovery performance can be improved, we need to investigate the pump recovery system in more detail, in particular the IL transfer characteristics.

When the power into the pump recovery system is reduced, ASE noise will be generated and added to the pump wave by the first EDFA. However, the pump wave will subsequently be filtered and the noise partly suppressed through the IL. This effectively makes the SL determine the noise generated and added to the pump through the pump recovery system. For our PSA/PIA-amplified link the noise on the recovered pump will impact the amplified signal through pump noise transfer in the PSA/PIA.

Also the transfer of phase modulation through the pump recovery system will depend on the power into the pump recovery system. The phase transfer through the IL is dependent on the field injected into the SL. Increased injection of ASE noise into the SL can therefore im-

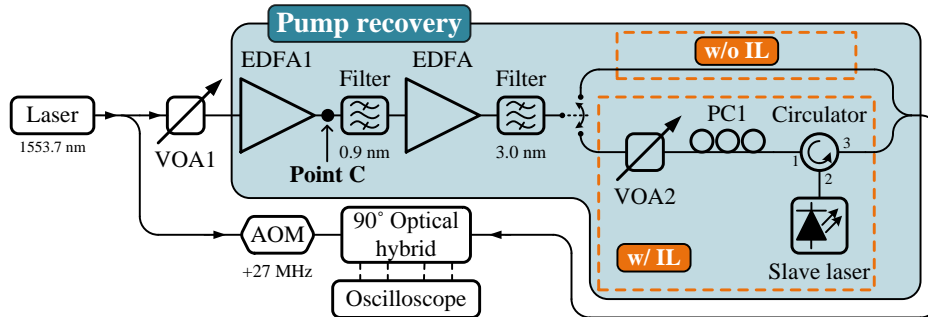


Fig. 5. Homodyne coherent detection setup used for characterizing noise generation in the pump recovery system and ASE noise transfer through the slave laser. VOA: variable optical attenuator, EDFA: erbium-doped fiber amplifier, PC: polarization controller, AOM: acousto-optic modulator, IL: injection locking.

pact and degrade the phase transfer. An obvious consequence of degraded phase transfer is reduced pump SBS suppression in the PSA/PIA which in turn can lead to a Q-factor penalty through pump noise transfer if the pump SBS becomes significant. For the PSA we also expect a degraded phase transfer to impact the PSA operation through misalignment of the phase-matching condition. If we denote the pump phase modulation at the pump recovery system input by θ_{in} and at the output by θ_{out} then the phase-matching condition in the PSA can be expressed as: $2\theta_p - \theta_s - \theta_i = \pi/2$ where $\theta_p = \theta'_p + \theta_{out}$ and $\theta_i = 2(\theta'_p + \theta_{in}) - \theta_s - \pi/2$. We see that if $\theta_{out} \neq \theta_{in}$, the phase-matching will be disturbed. A deviation from the phase-matching would translate into gain fluctuations which in turn would affect the output signal and cause a Q-factor penalty.

The discussion above implies that an understanding of the transfer characteristics of IL is crucial for explaining the performance of the pump recovery system. The transfer characteristics of an injection-locked DFB laser are highly dependent on parameters such as the injection ratio, defined as the ratio between the injected power and the SL output power, the frequency offset between the injected wave and the free running SL, and the SL driving current. Therefore, in order to identify the limiting factors in our pump recovery system, with our specific operating conditions, we need to measure the noise generation in the pump recovery system (and ASE noise transfer through the SL) as well as the phase modulation transfer through the pump recovery system.

3.1. Amplitude noise and phase noise generation

The noise generation in the pump recovery system was investigated using homodyne coherent detection and constellation analysis. The experimental setup is shown in Fig. 5. A wave at 1553.7 nm was split up into two branches; a signal branch and a local oscillator branch. The local oscillator branch was frequency shifted by 27 MHz using an acousto-optic modulator (AOM) and then passed into a 90° optical hybrid. The frequency was shifted in order to obtain a detectable beat tone between the local oscillator and the signal in the optical hybrid. The signal branch was passed through VOA1 for attenuation to vary the OSNR after EDFA1, i.e. at point C, and then into the pump recovery system.

Apart from removing the last EDFA, the pump recovery system was identical to the system used for the demonstration in section 2. We assumed that the last EDFA would not affect the noise properties of the recovered pump due to the high input power (20 dBm) to the EDFA from the SL. Both the case with and without IL in the pump recovery system was investigated,

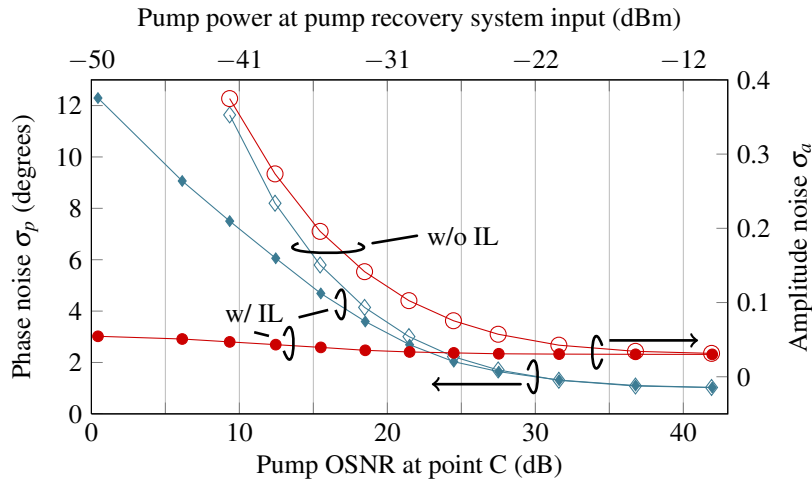


Fig. 6. Measured amplitude noise (right axis) and phase noise (left axis) after the pump recovery system with and without injection locking (IL) in the pump recovery system versus pump optical signal-to-noise ratio (OSNR) at point C (bottom axis) and pump power at the pump recovery system input (top axis). For the case with IL the slave laser input power was kept constant at -7.3 dBm, corresponding to an injection ratio of -27.3 dB.

as indicated in Fig. 5. As for the demonstration measurements the SL driving current was seven times the lasing threshold value and the wavelength was tuned so that the frequency difference between the SL and the incoming wave was minimized. The SOP into the SL was tuned using PC1 so that phase transfer of an incoming phase modulated wave was maximized. The SL input power was kept constant at a high value (-7.3 dBm, corresponding to an injection ratio of -27.3 dB) using VOA2 in order to reduce the effect of filtering in the SL, facilitating the measurement of broadband ASE noise transfer. At injected powers above -5 dBm the SL got over-modulated and spurious tones appeared, this regime was therefore avoided.

After the pump recovery system the wave was injected into the 90° optical hybrid. The hybrid output was detected using four 11 GHz bandwidth detectors and then sent to a real-time oscilloscope (16 GHz bandwidth) for sampling. The data was post-processed offline and amplitude noise and phase noise was extracted. The amplitude noise σ_a was defined as the standard deviation of the normalized amplitude and the phase noise σ_p was defined as the standard deviation of the phase.

Measured amplitude noise (right axis) and phase noise (left axis) at the output of the pump recovery system versus pump OSNR at point C (bottom axis) and pump power at the pump recovery system input (top axis) is presented in Fig. 6. For the case without IL both the amplitude noise and the phase noise increase with reduced pump OSNR, due to broadband ASE noise added by EDFA1. The noise floor reached at high pump OSNR was set by the sensitivity of the measurement system.

For the case with IL the amplitude noise is highly suppressed compared to the case without IL. The suppression of amplitude noise that we observe is in agreement with what was seen in [23]. However, we also observe a small increase in noise when the pump OSNR reach low values. Previous investigations of single frequency tone transfer through an injection-locked DFB laser help to explain the increase of amplitude noise. This occurs through FM-to-AM conversion and AM-to-AM transfer. It has been shown experimentally that FM-to-AM conversion is proportional to the modulation frequency up to the SL resonance frequency [24]. Due

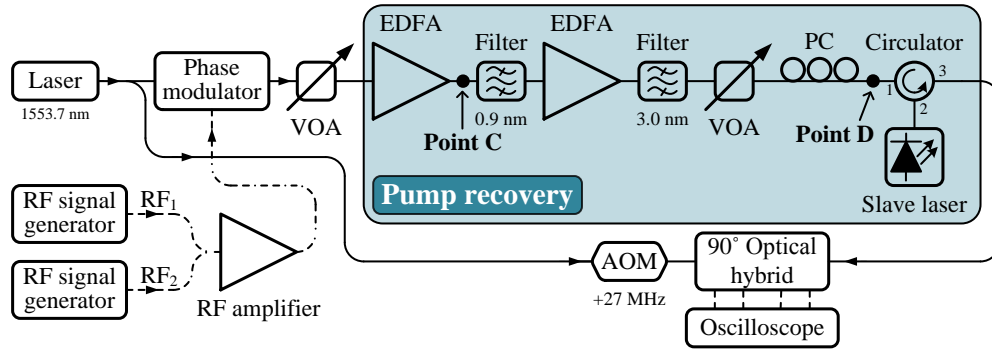


Fig. 7. Homodyne coherent detection setup used for characterizing phase transfer through the pump recovery system. VOA: variable optical attenuator, EDFA: erbium-doped fiber amplifier, PC: polarization controller, AOM: acousto-optic modulator, RF: radio frequency, IL: injection locking.

to the broadband nature of the ASE noise injected into the SL, only limited by the 0.9 nm bandpass filter after EDFA1, we can expect some impact of FM-to-AM conversion.

With IL the phase noise increases with decreased pump OSNR in a similar fashion as for the case without IL. It has been shown experimentally [25], and theoretically [24], that high FM-to-FM conversion should be expected up to several GHz under locking conditions similar to ours. However, since the ASE noise injected into the SL is broadband we expect some filtering through the SL, which is also what we see as reduced noise compared to the case without IL. The phase noise contribution from AM-to-FM conversion is expected to be negligible compared to the contribution from FM-to-FM transfer [23].

Based on our phase noise and amplitude noise measurements we can conclude that the performance improvement seen in Fig. 3 and Fig. 4 for the hybrid IL/EDFA pump recovery system compared to the EDFA-based system comes from the squeezing and filtering of amplitude noise and filtering of phase noise through the SL.

3.2. Phase modulation transfer degradation

The phase modulation transfer was investigated using an experimental setup similar to the one used for the noise measurements. The setup is shown in Fig. 7. In this case a phase modulator was placed before the pump recovery system and either one or two sinusoidal RF-tones were applied for transfer characterization. For the one tone case the frequency RF_1 was swept from 0.10 GHz to 2.30 GHz and the phase swing at the pump recovery system input $\Delta\phi_{in}$ was π . In the dual tone case the applied modulation was either $\{RF_1 = 0.10 \text{ GHz}, RF_2 = 0.32 \text{ GHz}\}$ or $\{RF_1 = 0.30 \text{ GHz}, RF_2 = 0.91 \text{ GHz}\}$. In this case the phase swing $\Delta\phi_{in}$ was 2π , each RF-tone contributing with π swing. The tone frequencies and amplitudes in the dual tone case were selected to produce a flat-top spectrum, since this is desirable for efficient SBS suppression [29]. The pump recovery system was tuned in the same way as for the noise measurements with the exception that also the SL input power was varied.

To determine the phase modulation transfer the sampled signal was filtered by 20 MHz bandpass filter(s) centered at the tone(s) center frequency in order to remove the noise contribution to the constellation. The phase modulation transfer ratio (MTR) was then calculated as the modulation depth at the output of the pump recovery system to that of the input

$$\text{Phase MTR} = \frac{\Delta\phi_{out}}{\Delta\phi_{in}} \quad (1)$$

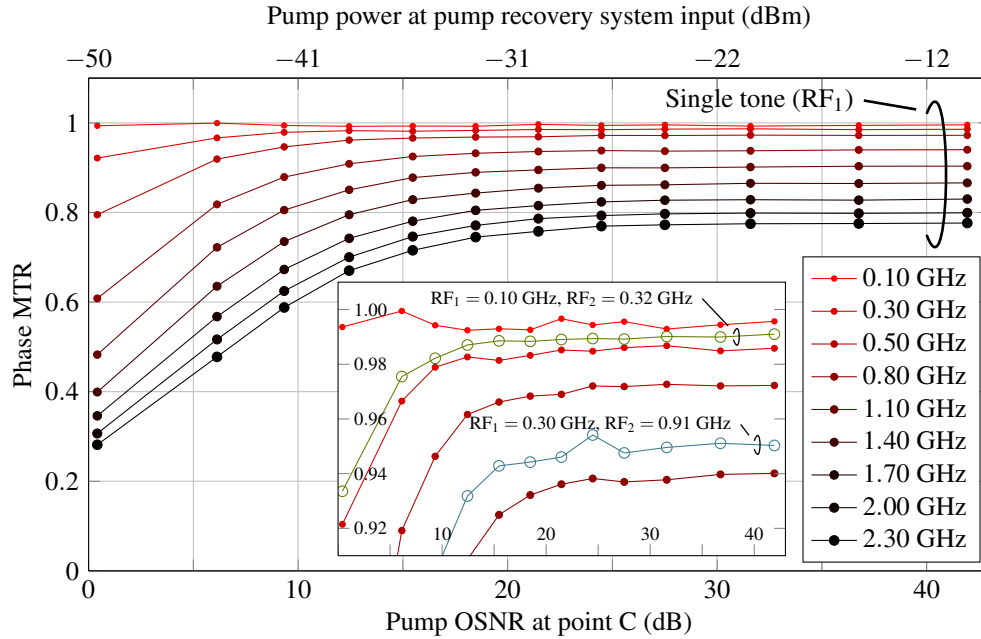


Fig. 8. Measured phase modulation transfer ratio (MTR) versus pump optical signal-to-noise ratio (OSNR) at point C (bottom axis) and pump power at the pump recovery system input (top axis) for various modulation frequencies, as given by the legend. The inset show the dual tone data together with the single tone data. The slave laser input power (power at point D) was kept at -7.6 dBm, corresponding to an injection ratio of -27.3 dB. RF: radio frequency.

where $\Delta\phi_{in} = \pi$ for the one tone case and $\Delta\phi_{in} = 2\pi$ for the two tone case.

We measured phase MTR versus pump OSNR at point C and phase MTR versus SL input power, i.e. power at point D. The measurement versus pump OSNR was done with high SL input power (-7.3 dBm, corresponding to an injection ratio of -27.3 dB) in order to minimize the transfer degradation due to the SL when studying the OSNR dependence. For the same reason the measurement versus SL input power was done with high pump OSNR (42 dB) at point C. Due to over-modulation and appearance of spurious tones the power injected into the SL was kept below -5 dBm.

Measured phase MTR versus pump OSNR at point C (bottom axis) and pump power at the pump recovery system input (top axis) is presented in Fig. 8. We see that the single tone phase MTR decrease with increased tone frequency. This is expected from the bandwidth of the FM-to-FM transfer in the SL [24]. We also see that for a fixed tone frequency the phase MTR decrease with decreased pump OSNR. This is due to the ASE noise injected into the SL. The inset show the dual tone data together with the single tone data. We note that the curves for the dual tone cases are located between the curves for the corresponding single tones. This is what to expect if the dual tone transfer is treated as independent transfer of the two single frequency tones. In particular we note that the dual tone case with $\{RF_1 = 0.10$ GHz, $RF_2 = 0.32$ GHz $\}$ is located between the curve for the single tone $RF_1 = 0.10$ GHz and the single tone $RF_1 = 0.30$ GHz.

Measured phase MTR versus SL input power is shown in Fig. 9. In Fig. 9, the single tone phase MTR decrease with increased tone frequency is again very clear. The phase MTR also

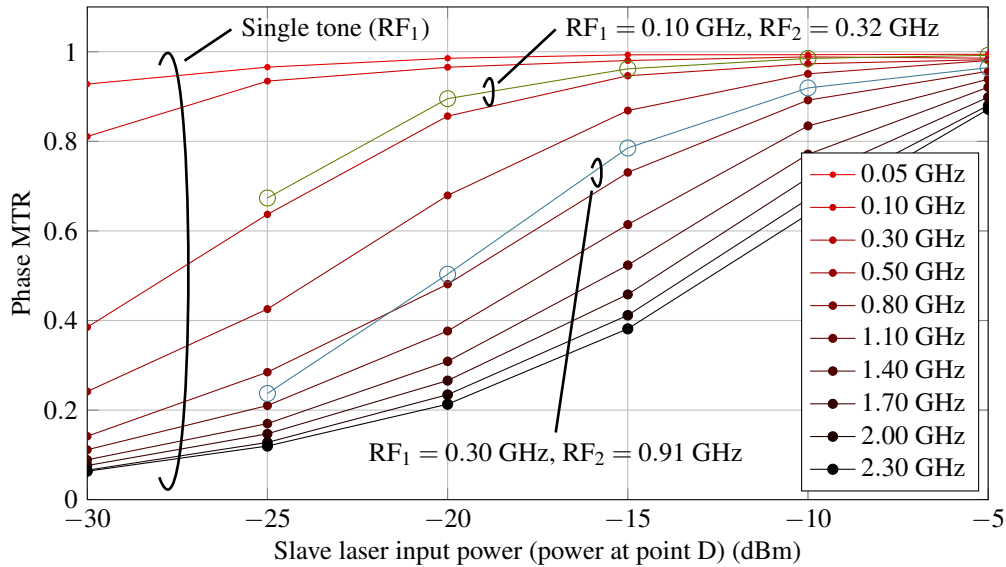


Fig. 9. Measured phase modulation transfer ratio (MTR) versus slave laser input power (power at point D) for various frequencies as given by the legends. The pump optical signal-to-noise ratio (OSNR) at point C was kept at 42 dB. RF: radio frequency.

decrease with reduced power into the SL. The reason for this is the decrease in FM-to-FM transfer bandwidth in the SL with reduced input power. The dual tone cases are located between the curves for the corresponding single tones. For the dual tone transfer, the tone with higher frequency will suffer more from the limited transfer bandwidth and thus the combined reduction in swing will be between the corresponding single tone cases.

Our measurements have shown that phase MTR is reduced, over all measured frequencies, both with reduced pump OSNR and reduced SL input power. The impact of reducing the SL input power was stronger than reducing the pump OSNR. They have also indicated that, from the perspective of phase MTR, dual tone transfer can be treated as independent transfer of two single tone components.

4. Characterization of pump recovery induced link penalty

The impact of noise generation and phase modulation transfer imperfection on the performance of the PSA/PIA-amplified link can be measured by varying the power into the pump recovery system and then extracting the resulting Q-factor penalty through analyzing the measured BER. By also varying the SL input power, for a fixed power into the pump recovery system, and comparing against the noise and phase transfer characteristics measured in section 3, we can gain additional information as to why these penalties arise.

The measurements were carried out using the same experimental setup as used for the demonstration in section 2, illustrated in Fig. 2. Apart from keeping the SL input power fixed, not tuned for lowest BER, the PSA/PIA-amplified link was operated in the same way as for the demonstration measurements. Two tones (0.1 GHz and 0.3 GHz) were used to phase modulate the pump in order to suppress pump SBS in the FOPAs.

The Q-factor penalty, extracted from measured BER, versus SL input power for various pump OSNR values is presented in Fig. 10. For the PSA-case the Q-factor penalty was taken with respect to the BER at -42 dBm received signal power, with high pump OSNR at point

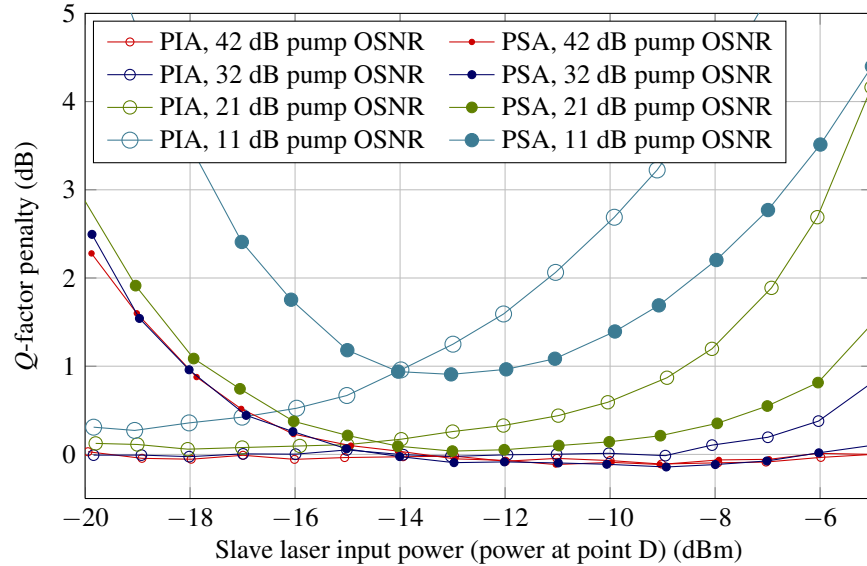


Fig. 10. Q-factor penalty calculated from measured bit error ratio versus slave laser input power (power at point D). The measurements were done at various pump optical signal-to-noise ratio (OSNR) at point C, as given by the legend. The phase-insensitive amplifier (PIA) gain and phase-sensitive amplifier (PSA) gain was kept at 20 dB.

A (42 dB) and high SL input power (-5 dBm). For the PIA-case the penalty was taken with respect to the BER at -37.5 dBm received signal power, also with high pump OSNR at point A (42 dB) and high SL input power (-5 dBm).

For the PIA-case there is a large Q-factor penalty at the combination of low pump OSNR and high SL input power. The penalty is reduced both with increased pump OSNR and reduced SL input power. The penalty reduction with increased pump OSNR is explained by the reduction of phase noise and amplitude noise generated in the pump recovery system, as shown in Fig. 6. The penalty reduction with reduced SL input power can be understood as follows. As the SL input power is reduced also the bandwidth of the FM-to-FM transfer is decreased, as seen in Fig. 9. In practice the SL will work as a phase bandpass filter centered at the pump frequency, with the bandwidth set by the FM-to-FM transfer bandwidth. Therefore, as the power into the SL is reduced more noise is filtered out and the penalty decrease. With reduced power into the SL (and reduced pump OSNR) the phase MTR is also reduced. Below about -20 dBm SL input power this lead to a sharp penalty onset due to pump SBS (not shown in Fig. 10).

In the PSA-case the Q-factor penalty curve is V-shaped at low pump OSNR (11 dB and 22 dB). In this case there are two effects influencing the penalty. The phase noise filtering in the SL is still an important effect but also the phase MTR is important, since that will impact the phase-matching in the PSA. The combined effect of these two factors, with phase noise giving penalty at high SL input powers (> -13 dBm for the 21 dB pump OSNR case) and phase-matching misalignment giving penalty at low SL input powers (< -13 dBm for the 21 dB pump OSNR case), give the V-shape. The measurement at 11 dB pump OSNR show higher penalty, both at low and high SL input powers, than the measurement at 22 dB pump OSNR since lower pump OSNR both introduce more noise and degrade the phase MTR, as seen in Fig. 6 and Fig. 8, respectively. For high pump OSNR (32 dB and 42 dB) there is no penalty at high SL input powers, i.e. there is no penalty due to phase noise. There is only a penalty at low

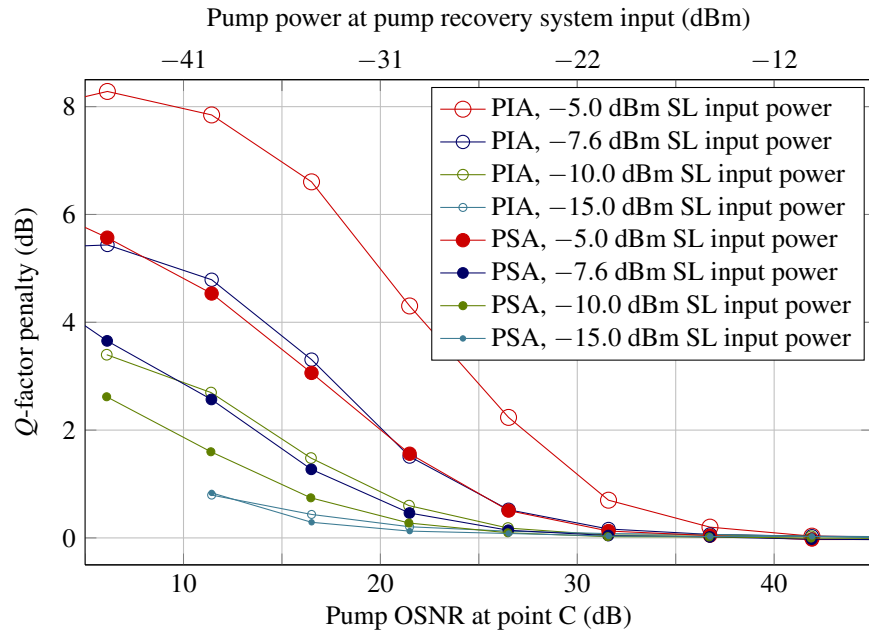


Fig. 11. Q-factor penalty calculated from measured bit error ratio versus pump optical signal-to-noise ratio (OSNR) at point C (bottom axis) and pump power at the pump recovery system input (top axis). The measurements were done at various slave laser input powers, as given by the legend. The phase-insensitive amplifier (PIA) gain and phase-sensitive amplifier (PSA) gain was kept at 20 dB.

SL input power (< -13 dBm) due to imperfect phase-matching in the PSA.

Finally, in Fig. 11 we show the Q-factor penalty versus pump OSNR at point C (bottom axis) and pump power at the pump recovery system input (top axis) for various SL input powers. The Q-factor penalty for the PSA-case was taken with respect to the BER at -42 dBm received signal power and for the PIA-case with respect to the BER at -37.5 dBm received signal power. In both cases with high pump OSNR at point A (45 dB) and high SL input power (-5 dBm). Measurements penalized by SBS, occurring at combined low pump OSNR and low SL input power, were removed from Fig. 11.

In Fig. 11 the impact of phase noise filtering through the SL is again very clear, when comparing curves at difference SL input power. The effect of imperfect phase-matching in the PSA is not clearly visible since the lowest SL input power presented is at -15 dBm, just marginally below the -13 dBm where we started to see the effect in Fig. 10. An interesting feature that is clearly visible is that the PSA-case show less Q-factor penalty than the PIA-case, i.e. the PSA is less sensitive to noise on the recovered pump than the PIA. The reason for this difference between the PSA-case and the PIA-case, also seen in Fig. 10, is not clear.

Based on the results shown in Fig. 10 we can deduce how large phase MTR is needed for penalty-free pump recovery operation in the PSA-amplified link. For high pump OSNR (32 dB and 42 dB) we saw a penalty onset due to low phase MTR at -13 dB SL input power. Referring to Fig. 9, that show phase MTR versus SL input power at 42 dB pump OSNR, we can relate the SL input power to a phase MTR value. In Fig. 9 we can read out that at a SL input power of -13 dBm the phase MTR is approximately 97% for the dual tone case or approximately 98% for the single $RF_1 = 0.10$ GHz tone and approximately 96% for the single $RF_1 = 0.30$ GHz

tone.

We can also deduce how much noise that can be tolerated for penalty-free pump recovery operation in the PSA- and PIA-amplified link. In Fig. 11 we see that the penalty onset is at about 25 dB pump OSNR for the PSA-case with -7.6 dBm SL input power. The corresponding value for the PIA-case is about 30 dB. In Fig. 6, showing the phase noise and amplitude noise versus pump OSNR at -7.3 dBm SL input power, we can read the corresponding phase noise and amplitude noise values. At 25 dB pump OSNR (the PSA-case penalty onset) the phase noise is 2.0 degrees and the amplitude noise is 0.03. At 30 dB pump OSNR (the PIA-case penalty onset) the phase noise is 1.4 degrees and the amplitude noise 0.03.

The penalty-free operating range for the pump recovery system could, for both the PSA- and PIA-amplified links, be extended to include lower pump OSNR values if lower bandwidth pump phase modulation was used. For the PIA-case this would mean that the SL input power could be reduced without introducing penalty from SBS, thus allowing for better noise filtering. For the PSA-case the effect would be that the penalty onset due to imperfect phase modulation transfer would move to lower SL input power which in turn would allow for lower SL input power and better noise filtering through the SL.

We can now explain the Q-factor penalty difference between the PIA- and PSA-case with IL seen at low pump OSNR values in Fig. 4. For the PIA system the penalty originate from SBS and for the PSA system the penalty is due to the combined effect of noise on the pump and imperfect phase-matching in the PSA.

Alternative SBS suppression techniques, not based on pump phase modulation, would improve the operating limits both in the PSA- and PIA-case since that would allow for lower bandwidth phase modulation of the pump or in the extreme case no pump phase modulation. In the case of no pump phase modulation we expect both the PSA and PIA system to be limited by in-band pump noise and the practical problem of keeping the frequency difference between the incoming pump and the SL within the IL locking bandwidth. However, we have not observed any penalty from in-band noise in the measurements we have presented here.

5. Conclusions

We have demonstrated and experimentally investigated a hybrid IL/EDFA-based pump recovery system for PSA-amplified links. Recovery of a pump wave, phase modulated by two sinusoidal RF-tones at 0.1 GHz and 0.3 GHz for SBS suppression, with 64 dB overall pump amplification, from -30 dBm to 34 dBm, is shown to have negligible penalty when measuring BER on a 10 GBd DQPSK signal transmitted through a PSA-amplified link. With the assumption of 10 dBm pump power launched into the fiber, this infers that the pump recovery system can handle up to 40 dB of pump attenuation. Theoretical estimates indicate that there will be no significant penalties associated with the pump recovery when replacing the 40 dB lumped loss with a 200 km dispersion compensated fiber span. Preliminary results have shown that even higher pump powers, up to 20 dBm, can be launched into the link without significant penalty [28]. This indicate that the pump recovery system could potentially handle even longer spans.

Measurements, based on homodyne coherent detection and constellation analysis, show that amplitude squeezing, amplitude noise filtering, and phase noise filtering through the SL can explain the superior performance of the hybrid IL/EDFA-based pump recovery system compared to a simple EDFA-based system. The measurements also showed that the phase MTR for the pump recovery system is reduced both with reduced SL input power, strong dependence, and with reduced pump OSNR, weaker dependence, and indicated that dual tone transfer can be treated as independent transfer of two single tones.

The impact of noise generation in and phase modulation transfer imperfections through the

pump recovery system on the performance of the PSA/PIA-amplified link was investigated and quantified. It was found that the PIA-amplified link is penalized directly by noise on the recovered pump wave and also by reduced phase MTR through reduced pump SBS suppression. The PSA-amplified link is penalized directly both by noise on the recovered pump and by degraded phase MTR. Our measurements show that a dual tone phase MTR of approximately 98% is needed to avoid penalty due to mismatch of the phase-matching condition in the PSA.

It is expected that lower bandwidth pump modulation would result in larger operating range for the pump recovery system, both in the PSA- and PIA-amplified link. If no tones had to be applied then we infer the operating range to be limited mainly by in-band pump noise and the practical problem of keeping the SL locked to the incoming pump wave. Our measurements also showed that the PSA-amplified link is less sensitive to noise on the recovered pump than the PIA-amplified link. However, we are not clear to why this is the case and further investigation is needed.

Our demonstrations have been carried out on a specific system transmitting single channel 10 GBd DQPSK data. However, we expect the pump recovery system operation to be independent of the number of channels and to a large extent on the modulation format of the transmitted data. Furthermore, the pump recovery system could be implemented in a multi-span scheme where one pump recovery system is included for each span. However, with cascaded pump recovery systems the accumulation of amplitude and phase noise as well as loss of phase modulation depth must be considered. According to Fig. 6 amplitude noise is heavily suppressed in the pump recovery system and should therefore not be accumulated in a cascaded scheme. Phase noise on the other hand will accumulate and eventually cause a penalty. Also the effect of non-ideal phase MTR will accumulate causing the phase modulation depth to be successively reduced, which will cause a penalty. Both the accumulation of phase noise and reduction of phase modulation depth can be decreased if the pump modulation bandwidth is reduced. Recent work has shown promising results towards achieving high-gain PSAs without pump phase modulation [31]. We expect that the presented results provide a viable path to enabling multi-span WDM compatible PSA-amplified transmission links over large spans.

Acknowledgements

This work was supported by the European Research Council Advanced Grant PSOPA (291618), by the Knut and Alice Wallenberg Foundation, and by the Swedish Research Council. The authors would like to thank OFS Fitel Denmark for providing the HNLFs.